EUROPEAN ORGANIZATION FOR NUCLEAR RESEARCH

LEPEWWG/TGC/2003-01
ALEPH 2003-016 CONF 2003-012
DELPHI 2003-068-PHYS-936
L3 Note 2826
OPAL TN-739
January 8, 2004

A Combination of Preliminary Results on Gauge Boson Couplings Measured by the LEP Experiments

The LEP Collaborations ALEPH, DELPHI, L3, OPAL, and the LEP TGC Working Group*

Prepared from contributions of the LEP experiments to the summer conferences 2003.

Abstract

This note presents a combination of published and preliminary measurements of triple gauge boson couplings (TGCs) and quartic gauge boson couplings (QGCs) from the four LEP experiments. We give an updated combination of the charged TGCs g_1^Z, κ_γ and λ_γ in single and multi-parameter fits. Updated results for the QGCs from the $ZZ\gamma\gamma$ vertex, a_c/Λ^2 and a_0/Λ^2, are given as well. The combinations of neutral TGCs h_i^V and f_i^V are also presented, including an updated f_i^V combination.

*Contact: Ulrich Parzefall, email: Ulrich.Parzefall@physik.uni-freiburg.de
The collaborations each take responsibility for the preliminary data of their own experiment.
WWW access at http://www.cern.ch/LEPEWWG/lepww/tgc/

1 Introduction

The measurement of gauge boson couplings and the search for possible anomalous contributions due to the effects of new physics beyond the Standard Model are among the principal physics aims at LEP-II [1]. Combined preliminary measurements of triple gauge boson couplings are presented here. Results from W-pair production are combined in single and two-parameter fits, including updated results from ALEPH, L3 and OPAL as well as an improved treatment of the main systematic effect in our previous combination, the uncertainty in the $O(\alpha_{em})$ correction. An updated combination of quartic gauge coupling (QGC) results for the $ZZ\gamma\gamma$ vertex is also presented, including data from ALEPH, L3 and OPAL. The combination of QGCs associated with the $WW\gamma\gamma$ vertex, including the sign convention as reported in [2, 3] and the reweighting based on [2] is foreseen for our next report. The combination of neutral TGCs measured in ZZ production (f-couplings) has been updated, including new results from L3 and OPAL. The combinations for neutral TGCs accessible through $Z\gamma$ production (h-couplings) reported in 2001 still remain valid [4].

The W-pair production process, $e^+e^- \to W^+W^-$, involves charged triple gauge boson vertices between the W^+W^- and the Z or photon. During LEP-II operation, about 10,000 W-pair events were collected by each experiment. Single W ($e\nu W$) and single photon ($\nu\bar{\nu}\gamma$) production at LEP are also sensitive to the $WW\gamma$ vertex. Results from these channels are also included in the combination for some experiments; the individual references should be consulted for details.

For the charged TGCs, Monte Carlo calculations (RacoonWW [5] and YFSWW [6]) incorporating an improved treatment of $O(\alpha_{em})$ corrections to the WW production have become our standard by now. The corrections affect the measurements of the charged TGCs in W-pair production. Results, some of them preliminary, including these $O(\alpha_{em})$ corrections have been submitted from all four LEP collaborations ALEPH [7], DELPHI [8], L3 [9] and OPAL [10]. LEP combinations are made for the charged TGC measurements in single- and two-parameter fits.

At centre-of-mass energies exceeding twice the Z boson mass, pair production of Z bosons is kinematically allowed. Here, one searches for the possible existence of triple vertices involving only neutral electroweak gauge bosons. Such vertices could also contribute to $Z\gamma$ production. In contrast to triple gauge boson vertices with two charged gauge bosons, purely neutral gauge boson vertices do not occur in the Standard Model of electroweak interactions.

Within the Standard Model, quartic electroweak gauge boson vertices with at least two charged gauge bosons exist. In e^+e^- collisions at LEP-II centre-of-mass energies, the $WWZ\gamma$ and $WW\gamma\gamma$ vertices contribute to $WW\gamma$ and $\nu\bar{\nu}\gamma\gamma$ production in s-channel and t-channel, respectively. The effect of the Standard Model quartic electroweak vertices is below the sensitivity of LEP-II. Quartic gauge boson vertices with only neutral bosons, like the $ZZ\gamma\gamma$ vertex, do not exist in the Standard Model. However, anomalous QGCs associated with this vertex are studied at LEP.

Anomalous quartic vertices are searched for in the production of $WW\gamma$, $\nu\bar{\nu}\gamma\gamma$ and $Z\gamma\gamma$ final states. The couplings related to the $ZZ\gamma\gamma$ and $WW\gamma\gamma$ vertices are assumed to be different [11], and are therefore treated separately. In this report, we only combine the results for the anomalous couplings associated with the $ZZ\gamma\gamma$ vertex. The combination of the $WW\gamma\gamma$ vertex couplings is foreseen for the near future.

1.1 Charged Triple Gauge Boson Couplings

The parametrisation of the charged triple gauge boson vertices is described in References [1, 12–17]. The most general Lorentz invariant Lagrangian which describes the triple gauge boson interaction has fourteen independent complex couplings, seven describing the WWγ vertex and seven describing the WWZ vertex. Assuming electromagnetic gauge invariance as well as C and P conservation, the number of independent TGCs reduces to five. A common set is $\{g_1^{\mathrm{Z}}, \kappa_{\mathrm{Z}}, \kappa_\gamma, \lambda_{\mathrm{Z}}, \lambda_\gamma\}$ where $g_1^{\mathrm{Z}} = \kappa_{\mathrm{Z}} = \kappa_\gamma = 1$ and $\lambda_{\mathrm{Z}} = \lambda_\gamma = 0$ in the Standard Model. The parameters proposed in [1] and used by the LEP experiments are g_1^{Z}, λ_γ and κ_γ with the gauge constraints:

$$\kappa_{\mathrm{Z}} = g_1^{\mathrm{Z}} - (\kappa_\gamma - 1)\tan^2\theta_{\mathrm{W}}\,, \tag{1}$$

$$\lambda_{\mathrm{Z}} = \lambda_\gamma\,, \tag{2}$$

where θ_W is the weak mixing angle. The couplings are considered as real, with the imaginary parts fixed to zero. In contrast to previous LEP combinations [4, 18], we are quoting the measured coupling values themselves and not their deviation from the Standard Model.

Note that the photonic couplings λ_γ and κ_γ are related to the magnetic and electric properties of the W-boson. One can write the lowest order terms for a multipole expansion describing the W-γ interaction as a function of λ_γ and κ_γ. For the magnetic dipole moment μ_W and the electric quadrupole moment q_W one obtains $e(1+\kappa_\gamma+\lambda_\gamma)/2m_{\mathrm{W}}$ and $-e(\kappa_\gamma-\lambda_\gamma)/m_{\mathrm{W}}^2$, respectively.

The inclusion of $O(\alpha_{em})$ corrections in the Monte Carlo calculations has a considerable effect on the charged TGC measurement. Both the total cross-section and the differential distributions are affected. The cross-section is reduced by 1-2% (depending on the energy). Amongst the differential distributions, the effects are naturally more complex. The polar W^- production angle carries most of the information on the TGC parameters; its shape is modified to be more forwardly peaked. In a fit to data, the $O(\alpha_{em})$ effect manifests itself as a negative shift of the obtained TGC values with a magnitude of typically -0.015 for λ_γ and g_1^{Z} and -0.04 for κ_γ.

1.2 Neutral Triple Gauge Boson Couplings

There are two classes of Lorentz invariant structures associated with neutral TGC vertices which preserve $U(1)_{em}$ and Bose symmetry, as described in [13, 19].

The first class refers to anomalous Z$\gamma\gamma^*$ and ZγZ* couplings which are accessible at LEP in the process $\mathrm{e^+e^-} \to \mathrm{Z}\gamma$. The parametrisation contains eight couplings: h_i^V with $i = 1, ..., 4$ and $V = \gamma$,Z. The superscript γ refers to Z$\gamma\gamma^*$ couplings and superscript Z refers to ZγZ* couplings. The photon and the Z boson in the final state are considered as on-shell particles, while the third boson at the vertex, the s-channel internal propagator, is off shell. The couplings h_1^V and h_2^V are CP-odd while h_3^V and h_4^V are CP-even.

The second class refers to anomalous ZZγ^* and ZZZ* couplings which are accessible at LEP-II in the process $\mathrm{e^+e^-} \to$ ZZ. This anomalous vertex is parametrised in terms of four couplings: f_i^V with $i = 4, 5$ and $V = \gamma$,Z. The superscript γ refers to ZZγ^* couplings and the superscript Z refers to ZZZ* couplings, respectively. Both Z bosons in the final state are assumed to be on-shell, while the third boson at the triple vertex, the s-channel internal propagator, is off-shell. The couplings f_4^V are CP-odd whereas f_5^V are CP-even.

The h_i^V and f_i^V couplings are assumed to be real and they vanish at tree level in the Standard Model.

1.3 Quartic Gauge Boson Couplings

The couplings associated with the two QGC vertices $WW\gamma\gamma$ and $ZZ\gamma\gamma$ are assumed to be different, and are by convention treated as separate couplings at LEP. In this report, we only combine QGCs related to the $ZZ\gamma\gamma$ vertex. The contribution of such anomalous quartic gauge boson couplings is described by two coupling parameters a_c/Λ^2 and a_0/Λ^2, which are zero in the Standard Model [20, 21]. Events from $\nu\bar{\nu}\gamma\gamma$ and $Z\gamma\gamma$ final states can originate from the $ZZ\gamma\gamma$ vertex and are therefore used to study anomalous QGCs.

2 Measurements

The combined results presented here are obtained from charged and neutral electroweak gauge boson coupling measurements, and from quartic gauge boson couplings measurements as discussed above. The individual references should be consulted for details about the data samples used.

The charged TGC analyses of ALEPH, DELPHI, L3 and OPAL use data collected at LEP-II up to centre-of-mass energies of 209 GeV. These analyses use different channels, typically the semileptonic and fully hadronic W-pair decays [7–10]. The full data set is analysed by ALEPH, L3 and OPAL, whereas DELPHI presently uses all data at 189 GeV and above. Anomalous TGCs affect both the total production cross-section and the shape of the differential cross-section as a function of the polar W^- production angle. The relative contributions of each helicity state of the W bosons are also changed, which in turn affects the distributions of their decay products. The analyses presented by each experiment make use of different combinations of each of these quantities. In general, however, all analyses use at least the expected variations of the total production cross-section and the W^- production angle. Results from $e\nu W$ and $\nu\bar{\nu}\gamma$ production are included by some experiments. Single W production is particularly sensitive to κ_γ, thus providing information complementary to that from W-pair production.

The h-coupling analyses of ALEPH, DELPHI and L3 use data collected up to centre-of-mass energies of 209 GeV. The OPAL measurements so far use the data at 189 GeV. The results of the f-couplings are obtained from the whole data set above the ZZ-production threshold by all of the experiments. The experiments already pre-combine different processes and final states for each of the couplings. For the neutral TGCs, the analyses use measurements of the total cross sections of $Z\gamma$ and ZZ production and the differential distributions: the h_i^V couplings [22–25] and the f_i^V couplings [22, 23, 26, 27] are determined.

The combination of quartic gauge boson couplings associated with the $ZZ\gamma\gamma$ vertex is at present based on analyses of ALEPH [28], L3 [29] and OPAL [30]. The L3 analysis uses data from the $q\bar{q}\gamma\gamma$ final state all at centre-of-mass energies above the Z resonance, from 130 GeV to 207 GeV. Both ALEPH and OPAL analyse the $\nu\bar{\nu}\gamma\gamma$ final state, with ALEPH using data from centre-of-mass energies ranging from 183 GeV to 209 GeV, and OPAL from 189 GeV to 209 GeV.

3 Combination Procedure

The combination is based on the individual likelihood functions from the four LEP experiments. Each experiment provides the negative log likelihood, $\log\mathcal{L}$, as a function of the coupling parameters to be combined. The single-parameter analyses are performed fixing all other parameters to their Standard Model values. The two-parameter analyses are performed setting the remaining parameters to their Standard Model values. For the charged TGCs, the gauge constraints listed in Section 1.1 are always enforced.

The $\log\mathcal{L}$ functions from each experiment include statistical as well as those systematic uncertainties which are considered as uncorrelated between experiments. For both single- and multi-parameter combinations, the individual $\log\mathcal{L}$ functions are combined. It is necessary to use the $\log\mathcal{L}$ functions directly in the combination, since in some cases they are not parabolic, and hence it is not possible to properly combine the results by simply taking weighted averages of the measurements.

The main contributions to the systematic uncertainties that are uncorrelated between experiments arise from detector effects, background in the selected signal samples, limited Monte Carlo statistics and the fitting method. Their importance varies for each experiment and the individual references should be consulted for details.

In the neutral TGC sector, the systematic uncertainties arising from the theoretical cross section prediction in Zγ-production ($\simeq 1\%$ in the $q\bar{q}\gamma$- and $\simeq 2\%$ in the $\nu\bar{\nu}\gamma$ channel) are treated as correlated. For ZZ production, the uncertainty on the theoretical cross section prediction is small compared to the statistical accuracy and therefore is neglected. Smaller sources of correlated systematic uncertainties, such as those arising from the LEP beam energy, are for simplicity treated as uncorrelated.

The combination procedure for neutral TGCs, where the relative systematic uncertainties are small, is unchanged with respect to the previous LEP combinations of electroweak gauge boson couplings [4, 18]. The correlated systematic uncertainties in the h-coupling analyses are taken into account by scaling the combined log-likelihood functions by the squared ratio of the sum of statistical and uncorrelated systematic uncertainty over the total uncertainty including all correlated uncertainties. For the general case of non-Gaussian probability density functions, this treatment of the correlated errors is only an approximation; it also neglects correlations in the systematic uncertainties between the parameters in multi-parameter analyses.

In the charged TGC sector, systematic uncertainties considered correlated between the experiments are the theoretical cross section prediction (0.5% for W-pair production and 5% for single W production), hadronisation effects, the final state interactions, namely Bose-Einstein correlations and colour reconnection, and the uncertainty in the radiative corrections themselves. The latter was the dominant systematic error in our previous combination, where we used a conservative estimate, the full effect from applying the $O(\alpha_{em})$ corrections. New preliminary analyses on the subject are now available from several LEP experiments [7], based on comparisons of fully simulated events using two different leading-pole approximation schemes (LPA-A and LPA-B) [31]. In addition, the availability of comparisons of both generators incorporating $O(\alpha_{em})$ corrections (RacoonWW and YFSWW [5,6]) makes it now possible to perform a more realistic estimation of this effect. In general, the TGC shift measured in the comparison of the two generators is found to be larger than the effect from the different LPA schemes. This improved estimation, whilst still being conservative, reduces the systematic uncertainty from $O(\alpha_{em})$ corrections by about a third for g_1^Z and λ_γ and roughly halves it for κ_γ, compared to the full $O(\alpha_{em})$ correction applied previously. The application of this reduced systematic error renders the charged TGC measurements statistics dominated.

In case of the charged TGCs, the systematic uncertainties considered correlated between the experiments amount to 58% of the combined statistical and uncorrelated uncertainties for λ_γ and g_1^Z, while for κ_γ it is 68%. This means that the measurements of λ_γ, g_1^Z and κ_γ are now clearly limited by statistics. An improved combination procedure [32] is used for the charged TGCs. This procedure allows the combination of statistical and correlated systematic uncertainties, independently of the analysis method chosen by the individual experiments.

The combination of charged TGCs uses the likelihood curves and correlated systematic errors submitted by each of the four experiments. The procedure is based on the introduction of an additional free parameter to take into account the systematic uncertainties, which are treated as shifts on the fitted TGC value, and are assumed to have a Gaussian distribution. A simultaneous minimisation of both parameters (TGC and systematic error) is performed to the log-likelihood function.

In detail, the combination proceeds in the following way: the set of measurements from the LEP experiments ALEPH, DELPHI, OPAL and L3 is given with statistical plus uncorrelated systematic uncertainties in terms of likelihood curves: $-\log\mathcal{L}^{A}_{stat}(x)$, $-\log\mathcal{L}^{D}_{stat}(x)$ $-\log\mathcal{L}^{L}_{stat}(x)$ and $-\log\mathcal{L}^{O}_{stat}(x)$, respectively, where x is the coupling parameter in question. Also given are the shifts for each of the five totally correlated sources of uncertainty mentioned above; each source S is leading to systematic errors σ^S_A, σ^S_D, σ^S_L and σ^S_O.

Additional parameters Δ^S are included in order to take into account a Gaussian distribution for each of the systematic uncertainties. The procedure then consists in minimising the function:

$$-\log\mathcal{L}_{total} = \sum_{E=A,D,L,O} \log\mathcal{L}^{E}_{stat}(x - \sum_{S=DPA,\sigma_{WW},HAD,BE,CR} (\sigma^S_E \Delta^S)) + \sum_S \frac{(\Delta^S)^2}{2} \qquad (3)$$

where x and Δ_S are the free parameters, and the sums run over the four experiments and the five systematic errors. The resulting uncertainty on x will take into account all sources of uncertainty, yielding a measurement of the coupling with the error representing statistical and systematic sources. The projection of the minima of the log-likelihood as a function of x gives the combined log-likelihood curve including statistical and systematic uncertainties. The advantage over the scaling method used previously is that it treats systematic uncertainties that are correlated between the experiments correctly, while not forcing the averaging of these systematic uncertainties into one global LEP systematics scaling factor. In other words, the (statistical) precision of each experiment now gets reduced by its own correlated systematic errors, instead of an averaged LEP systematic error. The method has been cross-checked against the scaling method, and was found to give comparable results. The inclusion of the systematic uncertainties lead to small differences as expected by the improved treatment of correlated systematic errors, a similar behaviour as seen in Monte Carlo comparisons of these two combinations methods [33]. Furthermore, it was shown that the minimisation-based combination method used for the charged TGCs agrees with the method based on optimal observables, where systematic effects are included directly in the mean values of the optimal observables (see [33]), for any realistic ratio of statistical and systematic uncertainties. Further details on the improved combination method can be found in [32].

In the combination of the QGCs, the influence of correlated systematic uncertainties is considered negligible compared to the statistical error, arising from the small number of selected events. Therefore, the QGCs are combined by adding the log-likelihood curves from the single experiments.

For all single- and multi-parameter results quoted in numerical form, the one standard deviation uncertainties (68% confidence level) are obtained by taking the coupling values for which $\Delta\log\mathcal{L} = +0.5$ above the minimum. The 95% confidence level (C.L.) limits are given by the coupling values for which $\Delta\log\mathcal{L} = +1.92$ above the minimum. Note that in the case of the neutral TGCs, double minima structures appear in the negative log-likelihood curves. For multi-parameter analyses, the two dimensional 68% C.L. contour curves for any pair of couplings are obtained by requiring $\Delta \log \mathcal{L} = +1.15$, while for the 95% C.L. contour curves $\Delta \log \mathcal{L} = +3.0$ is required. Since the results on the different parameters and parameter sets are obtained from the same data sets, they cannot be combined.

4 Results

We present results from the four LEP experiments on the various electroweak gauge boson couplings, and their combination. The charged TGC combination has been updated with the inclusion of recent results from ALEPH, L3 and OPAL. The neutral TGC results include an update of the f_i^V combinations, whilst the h_i^V combinations remain unchanged since our last note [4]. The results quoted for each individual experiment are calculated using the methods described in Section 3. Therefore they may differ slightly from those reported in the individual references, as the experiments in general use other methods to combine the data from different channels, and to include systematic uncertainties. In particular for the charged couplings, experiments using a combination method based on optimal observables (ALEPH, OPAL) obtain results with small differences compared to the values given by our combination technique. These small differences have been studied in Monte Carlo tests and are well understood [33]. For the h-coupling result from OPAL and DELPHI, a slightly modified estimate of the systematic uncertainty due to the theoretical cross section prediction is responsible for slightly different limits compared to the published results.

4.1 Charged Triple Gauge Boson Couplings

The individual analyses and results of the experiments for the charged couplings are described in [7–10].

Single-Parameter Analyses

The results of single-parameter fits from each experiment are shown in Table 1, where the errors include both statistical and systematic effects. The individual $\log \mathcal{L}$ curves and their sum are shown in Figure 1. The results of the combination are given in Table 2. A list of the systematic errors treated as fully correlated between the LEP experiments, and their shift on the combined fit result are given in Table 3.

Two-Parameter Analyses

Contours at 68% and 95% confidence level for the combined two-parameter fits are shown in Figure 2. The numerical results of the combination are given in Table 4. The errors include both statistical and systematic effects.

Parameter	ALEPH	DELPHI	L3	OPAL
g_1^Z	$1.026^{+0.034}_{-0.033}$	$1.002^{+0.038}_{-0.040}$	$0.928^{+0.042}_{-0.041}$	$0.985^{+0.035}_{-0.034}$
κ_γ	$1.022^{+0.073}_{-0.072}$	$0.955^{+0.090}_{-0.086}$	$0.922^{+0.071}_{-0.069}$	$0.929^{+0.085}_{-0.081}$
λ_γ	$0.012^{+0.033}_{-0.032}$	$0.014^{+0.044}_{-0.042}$	$-0.058^{+0.047}_{-0.044}$	$-0.063^{+0.036}_{-0.036}$

Table 1: The measured central values and one standard deviation errors obtained by the four LEP experiments. In each case the parameter listed is varied while the remaining two are fixed to their Standard Model values. Both statistical and systematic errors are included. The values given here differ slightly from the ones quoted in the individual contributions from the four LEP experiments, as a different combination method is used. See text in section 3 for details.

Parameter	68% C.L.	95% C.L.
g_1^Z	$0.991^{+0.022}_{-0.021}$	[0.949, 1.034]
κ_γ	$0.984^{+0.042}_{-0.047}$	[0.895, 1.069]
λ_γ	$-0.016^{+0.021}_{-0.023}$	[−0.059, 0.026]

Table 2: The combined 68% C.L. errors and 95% C.L. intervals obtained combining the results from the four LEP experiments. In each case the parameter listed is varied while the other two are fixed to their Standard Model values. Both statistical and systematic errors are included.

Source	g_1^Z	λ_γ	κ_γ
$O(\alpha_{em})$ correction	0.010	0.010	0.020
σ_{WW} prediction	0.003	0.005	0.014
Hadronisation	0.004	0.002	0.004
Bose-Einstein Correlation	0.005	0.004	0.009
Colour Reconnection	0.005	0.004	0.010
$\sigma_{singleW}$ prediction	-	-	0.011

Table 3: The systematic uncertainties considered correlated between the LEP experiments in the charged TGC combination and their effect on the combined fit results.

Parameter	68% C.L.	95% C.L.	Correlations	
g_1^Z	$1.004^{+0.024}_{-0.025}$	$[+0.954, \quad +1.050]$	1.00	+0.11
κ_γ	$0.984^{+0.049}_{-0.049}$	$[+0.894, \quad +1.084]$	+0.11	1.00
g_1^Z	$1.024^{+0.029}_{-0.029}$	$[+0.966, \quad +1.081]$	1.00	-0.40
λ_γ	$-0.036^{+0.029}_{-0.029}$	$[-0.093, \quad +0.022]$	-0.40	1.00
κ_γ	$1.026^{+0.048}_{-0.051}$	$[+0.928, \quad +1.127]$	1.00	+0.21
λ_γ	$-0.024^{+0.025}_{-0.021}$	$[-0.068, \quad +0.023]$	+0.21	1.00

Table 4: The measured central values, one standard deviation errors and limits at 95% confidence level, obtained by combining the four LEP experiments for the two-parameter fits of the charged TGC parameters. Since the shape of the log-likelihood is not parabolic, there is some ambiguity in the definition of the correlation coefficients and the values quoted here are approximate. The listed parameters are varied while the remaining one is fixed to its Standard Model value. Both statistical and systematic errors are included.

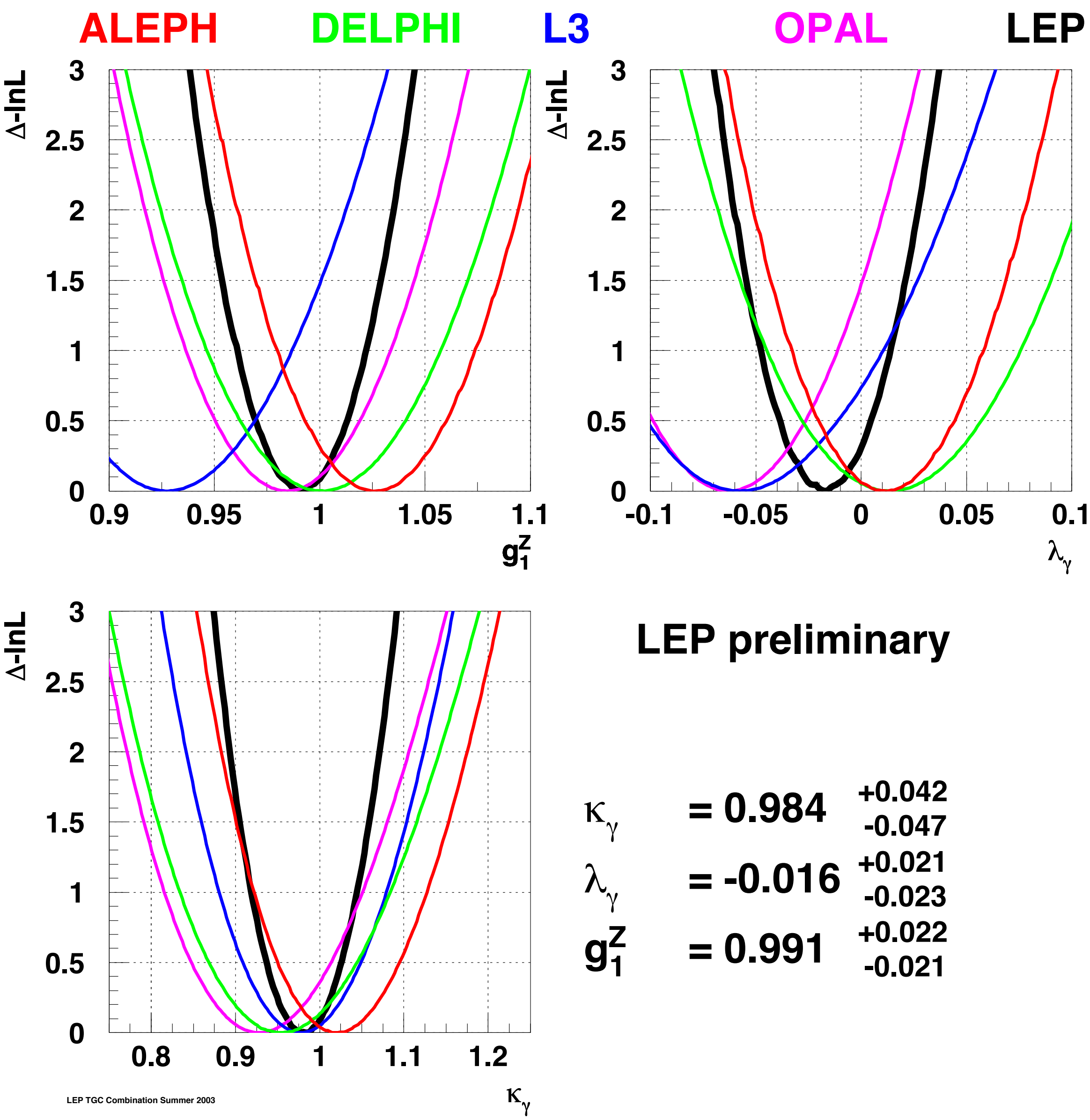

Figure 1: The $\log \mathcal{L}$ curves of the four experiments (thin lines) and the LEP combined curve (thick line) for the three charged TGCs g_1^Z, κ_γ and λ_γ. In each case, the minimal value is subtracted.

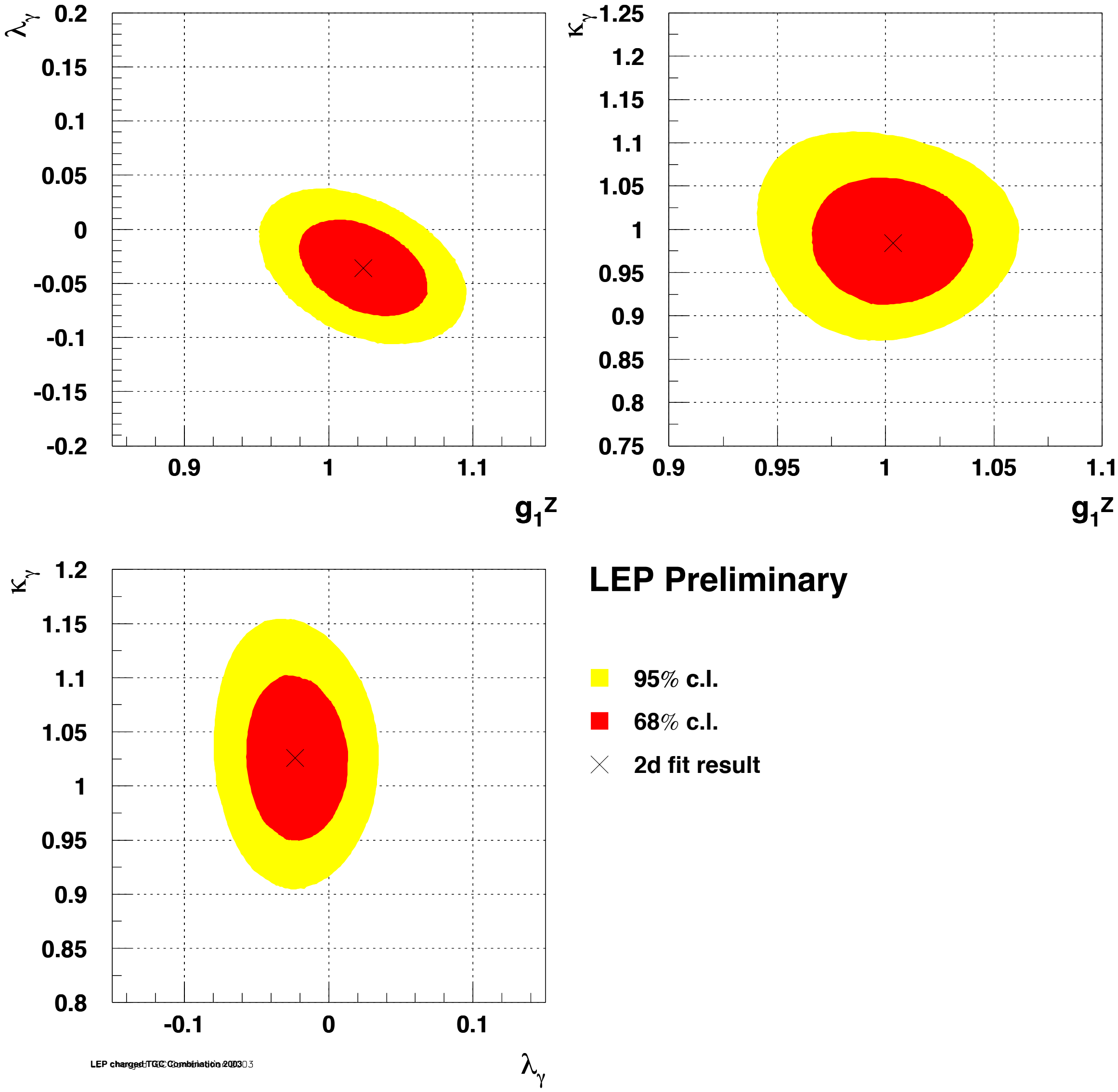

Figure 2: The 68% and 95% confidence level contours for the three two-parameter fits to the charged TGCs g_1^Z-λ_γ, g_1^Z-κ_γ and λ_γ-κ_γ. The fitted coupling value is indicated with a cross; the Standard Model value for each fit is in the centre of the grid. The contours include the contribution from systematic uncertainties.

4.2 Neutral Triple Gauge Boson Couplings in Zγ Production

The individual analyses and results of the experiments for the h-couplings are described in [22–25].

Single-Parameter Analyses

The results for each experiment are shown in Table 5, where the errors include both statistical and systematic uncertainties. The individual $\log\mathcal{L}$ curves and their sum are shown in Figures 3 and 4. The results of the combination are given in Table 6. From Figures 3 and 4 it is clear that the sensitivity of the L3 analysis [24] is the highest amongst the LEP experiments. This is partially due to the use of a larger phase space region, which increases the statistics by about a factor two, and partially due to additional information from using an optimal-observable technique.

Two-Parameter Analyses

The results for each experiment are shown in Table 7, where the errors include both statistical and systematic uncertainties. The 68% C.L. and 95% C.L. contour curves resulting from the combinations of the two-dimensional likelihood curves are shown in Figure 5. The LEP average values are given in Table 8.

Parameter	ALEPH	DELPHI	L3	OPAL
h_1^γ	$[-0.14, \quad +0.14]$	$[-0.15, \quad +0.15]$	$[-0.06, \quad +0.06]$	$[-0.13, \quad +0.13]$
h_2^γ	$[-0.07, \quad +0.07]$	$[-0.09, \quad +0.09]$	$[-0.053, \quad +0.024]$	$[-0.089, \quad +0.089]$
h_3^γ	$[-0.069, \quad +0.037]$	$[-0.047, \quad +0.047]$	$[-0.062, \quad -0.014]$	$[-0.16, \quad +0.00]$
h_4^γ	$[-0.020, \quad +0.045]$	$[-0.032, \quad +0.030]$	$[-0.004, \quad +0.045]$	$[+0.01, \quad +0.13]$
h_1^Z	$[-0.23, \quad +0.23]$	$[-0.24, \quad +0.25]$	$[-0.17, \quad +0.16]$	$[-0.22, \quad +0.22]$
h_2^Z	$[-0.12, \quad +0.12]$	$[-0.14, \quad +0.14]$	$[-0.10, \quad +0.09]$	$[-0.15, \quad +0.15]$
h_3^Z	$[-0.28, \quad +0.19]$	$[-0.32, \quad +0.18]$	$[-0.23, \quad +0.11]$	$[-0.29, \quad +0.14]$
h_4^Z	$[-0.10, \quad +0.15]$	$[-0.12, \quad +0.18]$	$[-0.08, \quad +0.16]$	$[-0.09, \quad +0.19]$

Table 5: The 95% C.L. intervals ($\Delta\log\mathcal{L} = 1.92$) measured by the ALEPH, DELPHI, L3 and OPAL. In each case the parameter listed is varied while the remaining ones are fixed to their Standard Model values. Both statistical and systematic uncertainties are included.

Parameter	95% C.L.
h_1^γ	$[-0.056, \quad +0.055]$
h_2^γ	$[-0.045, \quad +0.025]$
h_3^γ	$[-0.049, \quad -0.008]$
h_4^γ	$[-0.002, \quad +0.034]$
h_1^Z	$[-0.13, \quad +0.13]$
h_2^Z	$[-0.078, \quad +0.071]$
h_3^Z	$[-0.20, \quad +0.07]$
h_4^Z	$[-0.05, \quad +0.12]$

Table 6: The 95% C.L. intervals ($\Delta \log \mathcal{L} = 1.92$) obtained combining the results from the four experiments. In each case the parameter listed is varied while the remaining ones are fixed to their Standard Model values. Both statistical and systematic uncertainties are included.

Parameter	ALEPH	DELPHI	L3
h_1^γ	$[-0.32, \quad +0.32]$	$[-0.28, \quad +0.28]$	$[-0.17, \quad +0.04]$
h_2^γ	$[-0.18, \quad +0.18]$	$[-0.17, \quad +0.18]$	$[-0.12, \quad +0.02]$
h_3^γ	$[-0.17, \quad +0.38]$	$[-0.48, \quad +0.20]$	$[-0.09, \quad +0.13]$
h_4^γ	$[-0.08, \quad +0.29]$	$[-0.08, \quad +0.15]$	$[-0.04, \quad +0.11]$
h_1^Z	$[-0.54, \quad +0.54]$	$[-0.45, \quad +0.46]$	$[-0.48, \quad +0.33]$
h_2^Z	$[-0.29, \quad +0.30]$	$[-0.29, \quad +0.29]$	$[-0.30, \quad +0.22]$
h_3^Z	$[-0.58, \quad +0.52]$	$[-0.57, \quad +0.38]$	$[-0.43, \quad +0.39]$
h_4^Z	$[-0.29, \quad +0.31]$	$[-0.31, \quad +0.28]$	$[-0.23, \quad +0.28]$

Table 7: The 95% C.L. intervals ($\Delta \log \mathcal{L} = 1.92$) measured by ALEPH, DELPHI and L3. In each case the two parameters listed are varied while the remaining ones are fixed to their Standard Model values. Both statistical and systematic uncertainties are included.

Parameter	95% C.L.	Correlations	
h_1^γ	$[-0.16, \quad +0.05]$	1.00	+0.79
h_2^γ	$[-0.11, \quad +0.02]$	+0.79	1.00
h_3^γ	$[-0.08, \quad +0.14]$	1.00	+0.97
h_4^γ	$[-0.04, \quad +0.11]$	+0.97	1.00
h_1^Z	$[-0.35, \quad +0.28]$	1.00	+0.77
h_2^Z	$[-0.21, \quad +0.17]$	+0.77	1.00
h_3^Z	$[-0.37, \quad +0.29]$	1.00	+0.76
h_4^Z	$[-0.19, \quad +0.21]$	+0.76	1.00

Table 8: The 95% C.L. intervals ($\Delta \log \mathcal{L} = 1.92$) obtained combining the results from ALEPH, DELPHI and L3. In each case the two parameters listed are varied while the remaining ones are fixed to their Standard Model values. Both statistical and systematic uncertainties are included. Since the shape of the log-likelihood is not parabolic, there is some ambiguity in the definition of the correlation coefficients and the values quoted here are approximate.

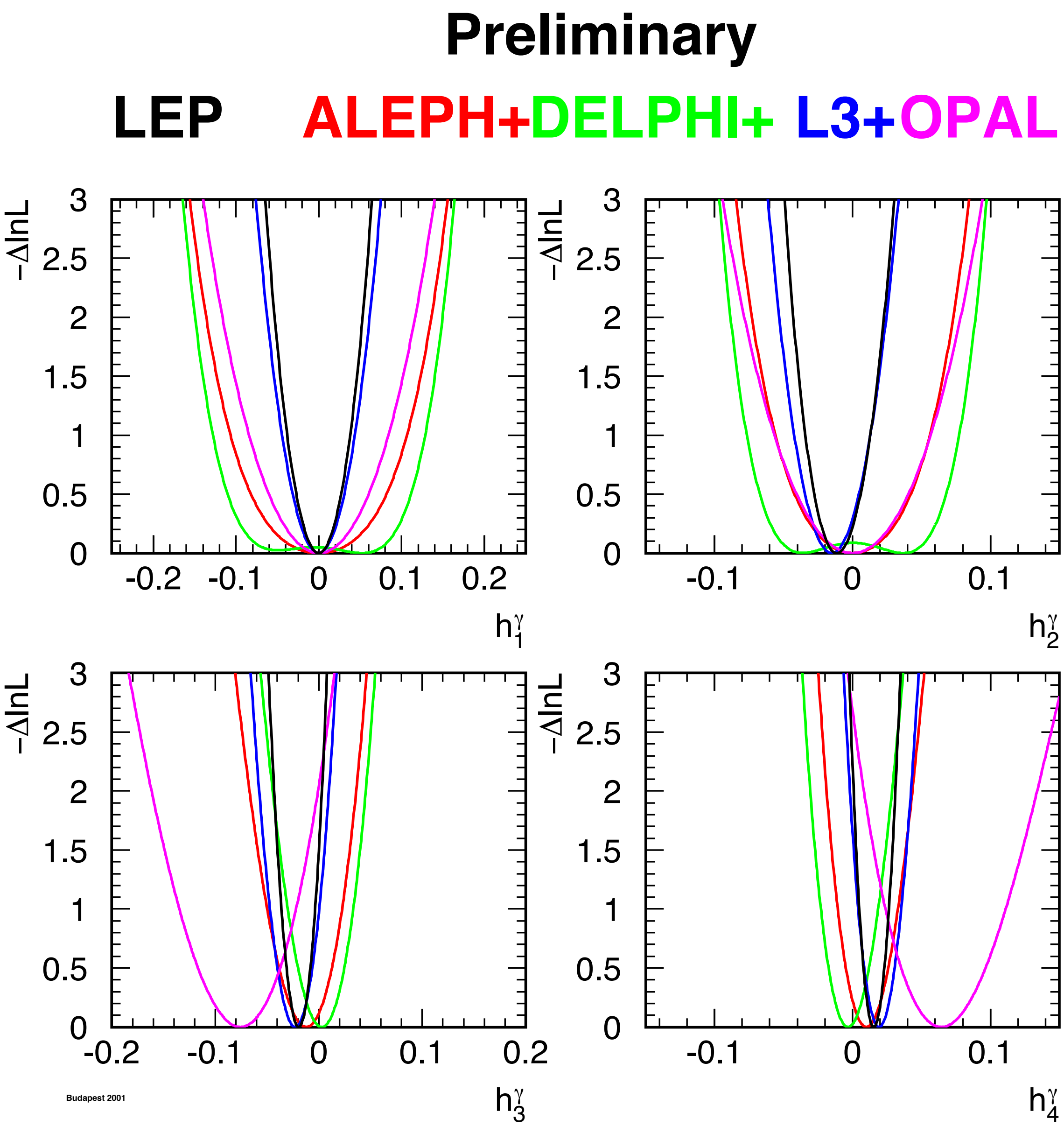

Figure 3: The $\log \mathcal{L}$ curves of the four experiments, and the LEP combined curve for the four neutral TGCs h_i^γ, $i = 1, 2, 3, 4$. In each case, the minimal value is subtracted.

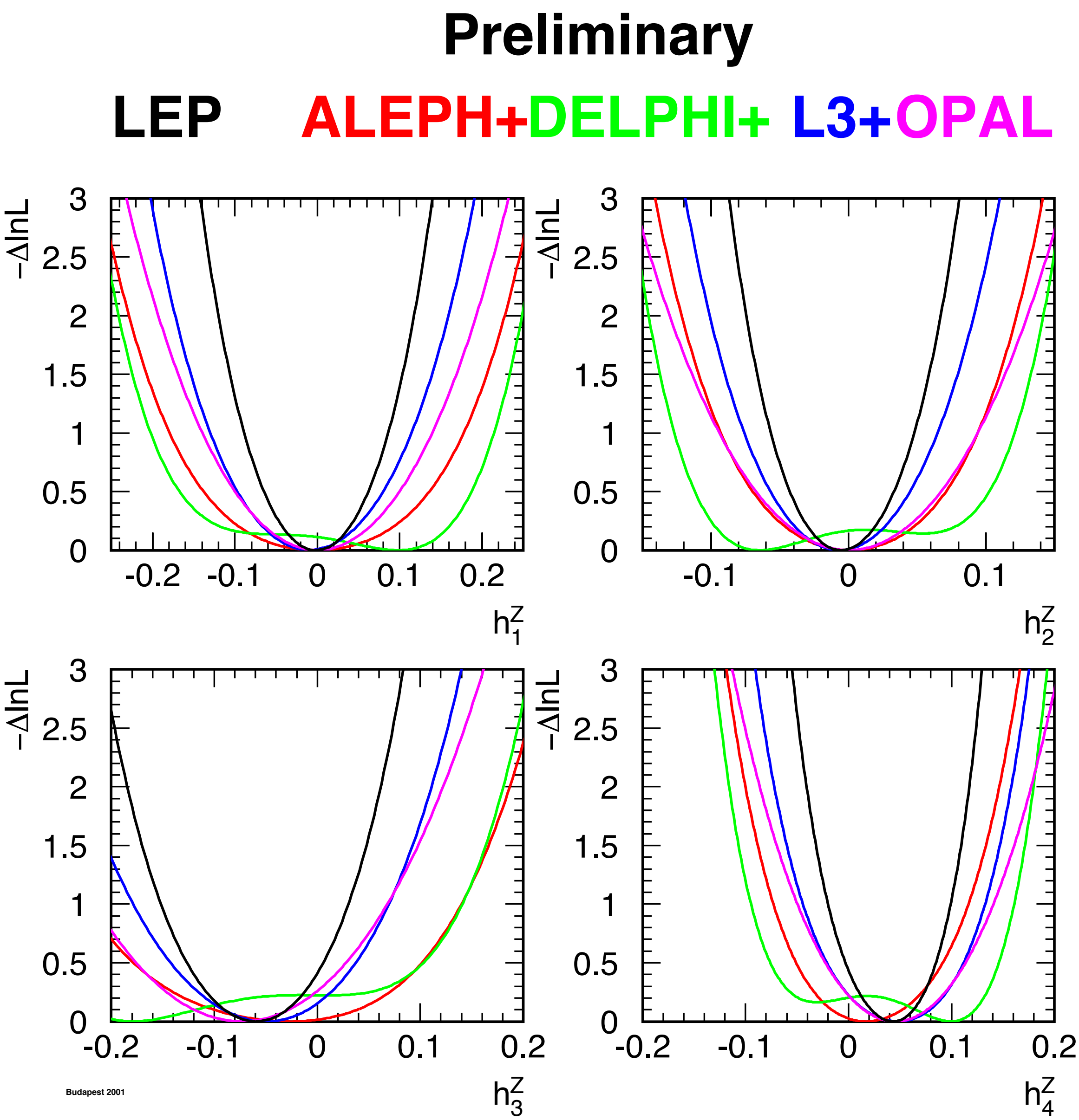

Figure 4: The $\log\mathcal{L}$ curves of the four experiments, and the LEP combined curve for the four neutral TGCs h_i^Z, $i = 1, 2, 3, 4$. In each case, the minimal value is subtracted.

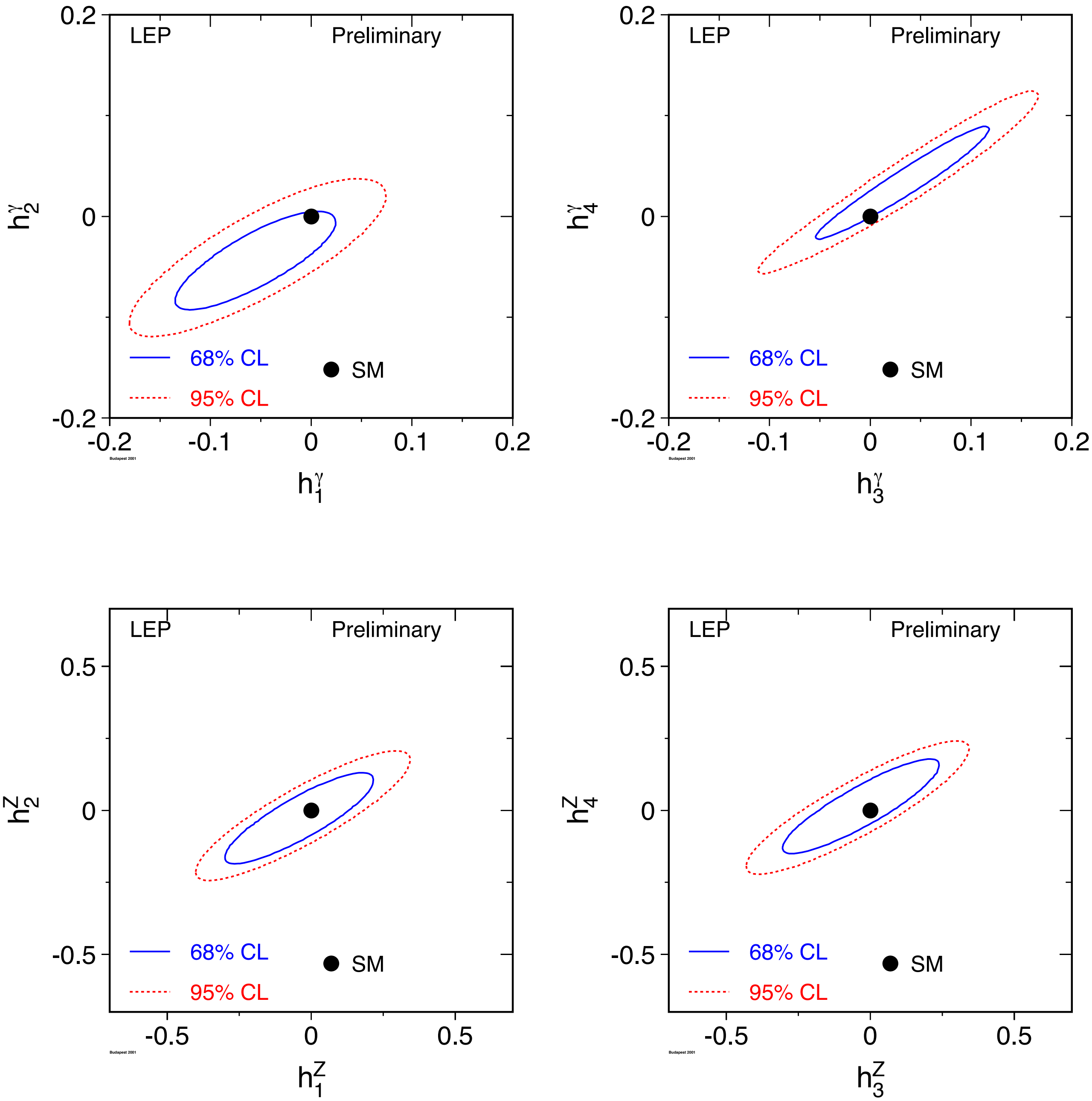

Figure 5: Contour curves of 68% C.L. and 95% C.L. in the planes (h_1^γ, h_2^γ), (h_3^γ, h_4^γ), (h_1^Z, h_2^Z) and (h_3^Z, h_4^Z) showing the LEP combined result.

4.3 Neutral Triple Gauge Boson Couplings in ZZ Production

The individual analyses and results of the experiments for the f-couplings are described in [22, 23, 26, 27].

Single-Parameter Analyses

The results for each experiment are shown in Table 9, where the errors include both statistical and systematic uncertainties. The individual $\log \mathcal{L}$ curves and their sum are shown in Figure 6. The results of the combination are given in Table 10.

Two-Parameter Analyses

The results from each experiment are shown in Table 11, where the errors include both statistical and systematic uncertainties. The 68% C.L. and 95% C.L. contour curves resulting from the combinations of the two-dimensional likelihood curves are shown in Figure 7. The LEP average values are given in Table 12.

Parameter	ALEPH	DELPHI	L3	OPAL
f_4^γ	$[-0.26, \quad +0.26]$	$[-0.26, \quad +0.28]$	$[-0.28, \quad +0.28]$	$[-0.32, \quad +0.33]$
f_4^Z	$[-0.44, \quad +0.43]$	$[-0.49, \quad +0.42]$	$[-0.48, \quad +0.46]$	$[-0.45, \quad +0.58]$
f_5^γ	$[-0.54, \quad +0.56]$	$[-0.48, \quad +0.61]$	$[-0.39, \quad +0.47]$	$[-0.71, \quad +0.59]$
f_5^Z	$[-0.73, \quad +0.83]$	$[-0.42, \quad +0.69]$	$[-0.35, \quad +1.03]$	$[-0.94, \quad +0.25]$

Table 9: The 95% C.L. intervals ($\Delta \log \mathcal{L} = 1.92$) measured by ALEPH, DELPHI, L3 and OPAL. In each case the parameter listed is varied while the remaining ones are fixed to their Standard Model values. Both statistical and systematic uncertainties are included.

Parameter	95% C.L.
f_4^γ	$[-0.17, \quad +0.19]$
f_4^Z	$[-0.30, \quad +0.30]$
f_5^γ	$[-0.32, \quad +0.36]$
f_5^Z	$[-0.34, \quad +0.38]$

Table 10: The 95% C.L. intervals ($\Delta \log \mathcal{L} = 1.92$) obtained combining the results from all four experiments. In each case the parameter listed is varied while the remaining ones are fixed to their Standard Model values. Both statistical and systematic uncertainties are included.

Parameter	ALEPH	DELPHI	L3	OPAL
f_4^γ	$[-0.26, \quad +0.26]$	$[-0.26, \quad +0.28]$	$[-0.28, \quad +0.28]$	$[-0.32, \quad +0.33]$
f_4^Z	$[-0.44, \quad +0.43]$	$[-0.49, \quad +0.42]$	$[-0.48, \quad +0.46]$	$[-0.47, \quad +0.58]$
f_5^γ	$[-0.52, \quad +0.53]$	$[-0.52, \quad +0.61]$	$[-0.52, \quad +0.62]$	$[-0.67, \quad +0.62]$
f_5^Z	$[-0.77, \quad +0.86]$	$[-0.44, \quad +0.69]$	$[-0.47, \quad +1.39]$	$[-0.95, \quad +0.33]$

Table 11: The 95% C.L. intervals ($\Delta \log \mathcal{L} = 1.92$) measured by ALEPH, DELPHI, L3 and OPAL. In each case the two parameters listed are varied while the remaining ones are fixed to their Standard Model values. Both statistical and systematic uncertainties are included.

Parameter	95% C.L.	Correlations	
f_4^γ	$[-0.17, \quad +0.19]$	1.00	0.07
f_4^Z	$[-0.30, \quad +0.29]$	0.07	1.00
f_5^γ	$[-0.34, \quad +0.38]$	1.00	-0.17
f_5^Z	$[-0.38, \quad +0.36]$	-0.17	1.00

Table 12: The 95% C.L. intervals ($\Delta \log \mathcal{L} = 1.92$) obtained combining the results from all four experiments. In each case the two parameters listed are varied while the remaining ones are fixed to their Standard Model values. Both statistical and systematic uncertainties are included. Since the shape of the log-likelihood is not parabolic, there is some ambiguity in the definition of the correlation coefficients and the values quoted here are approximate.

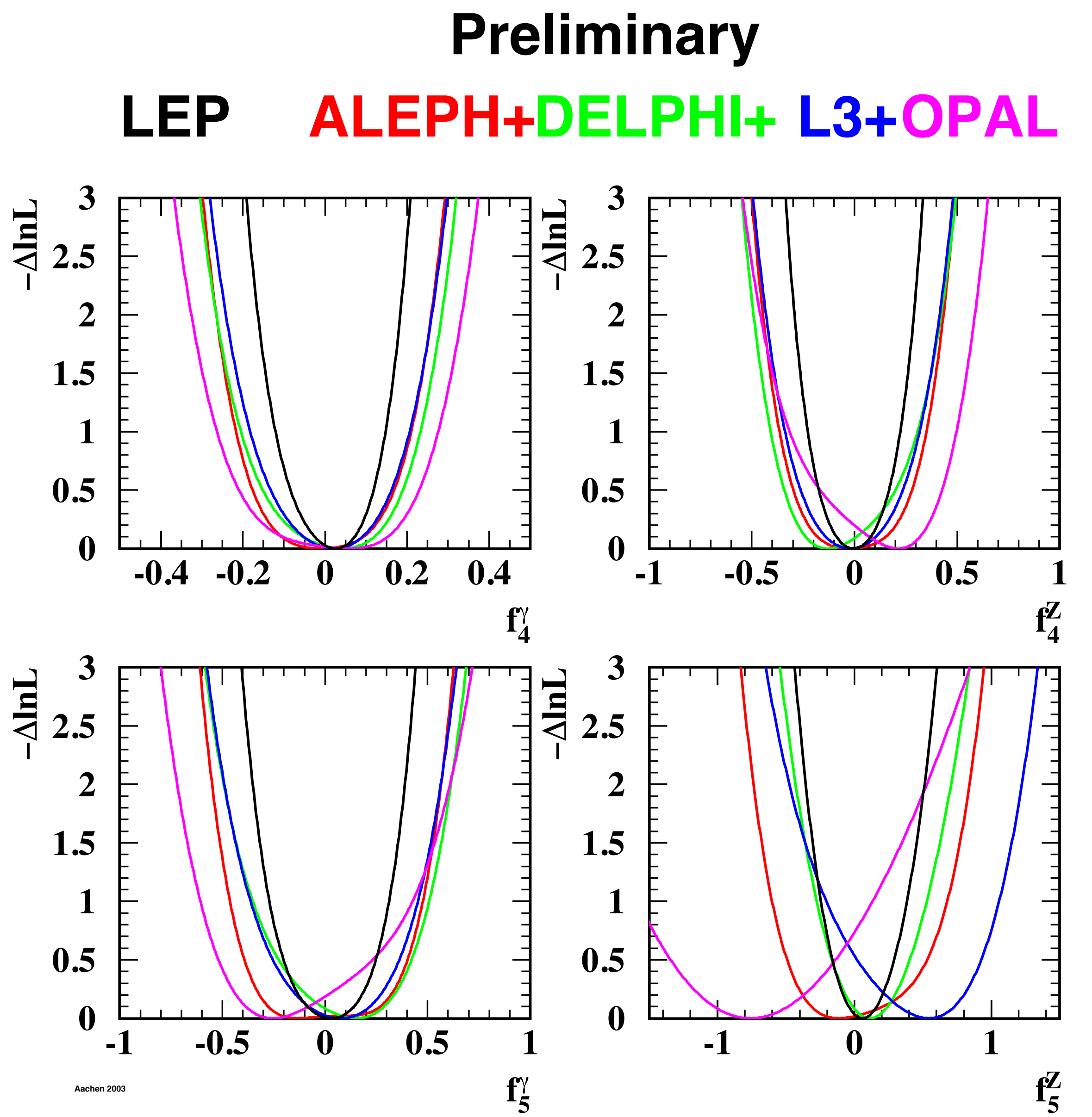

Figure 6: The $\log\mathcal{L}$ curves of the four experiments, and the LEP combined curve for the four neutral TGCs f_i^V, $V = \gamma, Z$, $i = 4, 5$. In each case, the minimal value is subtracted.

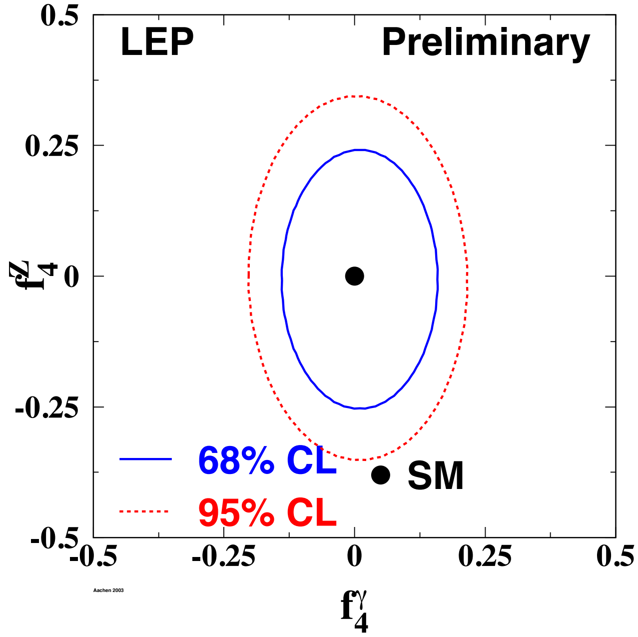

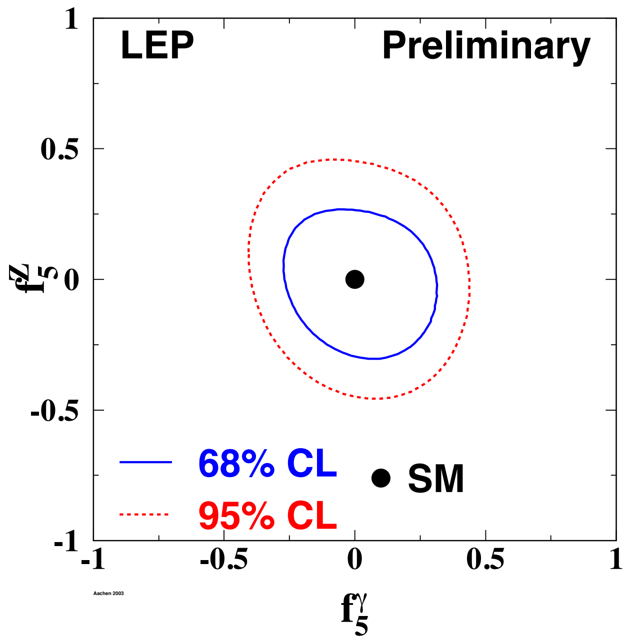

Figure 7: Contour curves of 68% C.L. and 95% C.L. in the plane (f_4^γ, f_4^Z) and (f_5^γ, f_5^Z) showing the LEP combined result.

4.4 Quartic Gauge Boson Couplings

The individual numerical results from the experiments participating in the combination, and the combined result are shown in Table 13. The corresponding $\log \mathcal{L}$ curves are shown in Figure 8. The errors include both statistical and systematic uncertainties.

Parameter	ALEPH	L3	OPAL	Combined
a_c/Λ^2	$[-0.041, \quad +0.044]$	$[-0.037, \quad +0.054]$	$[-0.045, \quad +0.050]$	$[-0.029, \quad +0.039]$
a_0/Λ^2	$[-0.012, \quad +0.019]$	$[-0.014, \quad +0.027]$	$[-0.012, \quad +0.031]$	$[-0.008, \quad +0.021]$

Table 13: The limits for the QGCs a_c/Λ^2 and a_0/Λ^2 associated with the $ZZ\gamma\gamma$ vertex at 95% confidence level for ALEPH, L3 and OPAL, and the LEP result obtained by combining them. Both statistical and systematic errors are included.

Conclusions

Combinations of charged and neutral triple gauge boson couplings, as well as quartic gauge boson couplings associated with the $ZZ\gamma\gamma$ vertex were made, based on results from the four LEP experiments ALEPH, DELPHI, L3 and OPAL. No significant deviation from the Standard Model prediction is seen for any of the electroweak gauge boson couplings studied. With the LEP-combined charged TGC results, the existence of triple gauge boson couplings among the electroweak gauge bosons is experimentally verified. As an example, these data allow the Kaluza-Klein theory [34], in which $\kappa_\gamma = -2$, to be excluded completely [35].

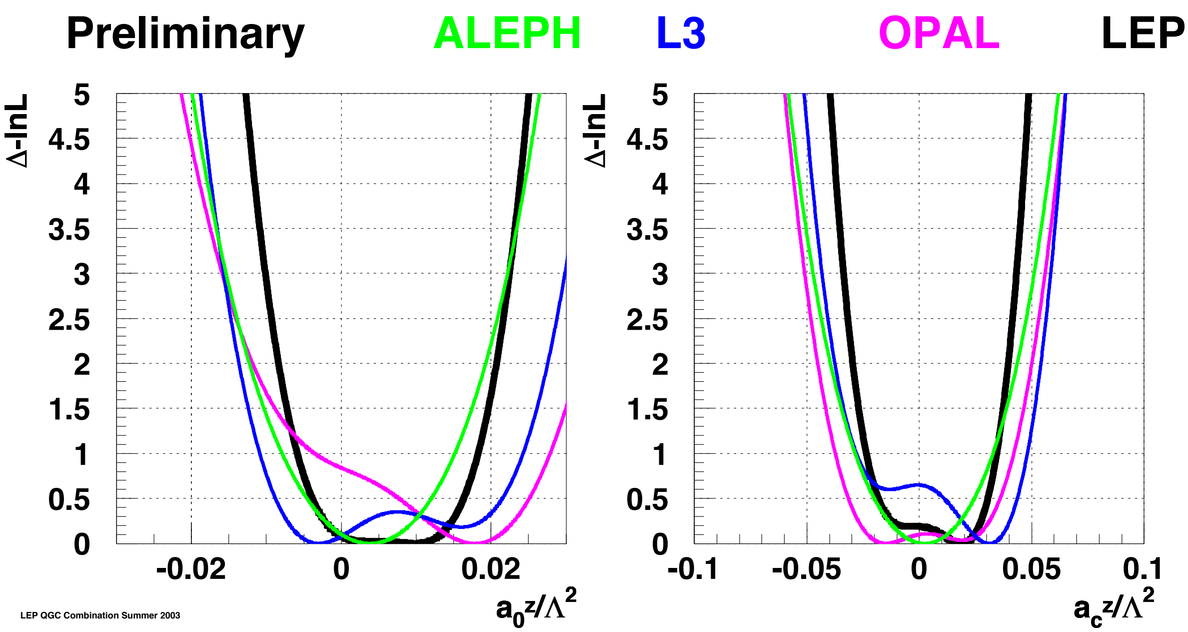

Figure 8: The $\log \mathcal{L}$ curves of L3 and OPAL (thin lines) and the combined curve (thick line) for the QGCs a_c/Λ^2 and a_0/Λ^2, associated with the ZZ$\gamma\gamma$ vertex. In each case, the minimal value is subtracted.

References

[1] G. Gounaris *et al.*, in *Physics at LEP 2*, Report CERN 96-01 (1996), eds G. Altarelli, T. Sjöstrand, F. Zwirner, Vol. 1, p. 525.

[2] G. Montagna *et al.*, Phys. Lett. **B515** (2001) 197–205.

[3] A. Denner *et al.*, Eur. Phys. J. **C 20** (2001) 201.

[4] The LEP-TGC combination group, LEPEWWG/TGC/2001-03, September 2001.

[5] A. Denner, S. Dittmaier, M. Roth and D. Wackeroth, Nucl. Phys. **B560** (1999) 33.
A. Denner, S. Dittmaier, M. Roth and D. Wackeroth, Nucl. Phys. **B587** (2000) 67.
A. Denner, S. Dittmaier, M. Roth and D. Wackeroth, Phys. Lett. **B475** (2000) 127.
A. Denner, S. Dittmaier, M. Roth and D. Wackeroth, hep-ph/0101257.
The RACOONWW cross-sections at 155–215 GeV have been kindly provided by the authors.

[6] S. Jadach, W. Płaczek, M. Skrzypek, B.F.L. Ward, Phys. Rev. **D54** (1996) 5434.
S. Jadach, W. Płaczek, M. Skrzypek, B.F.L. Ward, Z. Wąs, Phys. Lett. **B417** (1998) 326.
S. Jadach, W. Płaczek, M. Skrzypek, B.F.L. Ward, Z. Wąs, Phys. Rev. **D61** (2000) 113010.
S. Jadach, W. Płaczek, M. Skrzypek, B.F.L. Ward, Z. Wąs, preprint CERN-TH/2000-337, hep-ph/0007012; submitted to Phys. Lett. B.
S. Jadach, W. Płaczek, M. Skrzypek, B.F.L. Ward, Z. Wąs, Comput. Phys. Commun. **140** (2001) 432.
The YFSWW cross-sections at 155–215 GeV have been kindly provided by the authors.

[7] ALEPH Collaboration, *Measurement of Triple Gauge-Boson Couplings in e^+e^- collisions from 183 to 209GeV*, ALEPH 2003-015 CONF 2003-011.

[8] DELPHI Collaboration, *Measurement of Charged Trilinear Gauge Boson Couplings* , DELPHI 2003-051 (July 2003) CONF-671.

[9] L3 Collaboration, *Preliminary Results on the Measurement of Triple-Gauge-Boson Couplings of the W Boson at LEP*, L3 Note 2820 (September 2003).

[10] OPAL Collaboration, *Measurement of charged current triple gauge boson couplings using W pairs at LEP*, submitted to Eur. Phys. J. C., CERN-EP 2003-042, hep-ex/0308067.

[11] G. Bélanger *et al.*, Eur. Phys. J. **C 13** (2000) 283.

[12] K. Gaemers and G. Gounaris, Z. Phys. **C 1** (1979) 259.

[13] K. Hagiwara *et al.*, Nucl. Phys. **B282** (1987) 253.

[14] K. Hagiwara, S. Ishihara, R. Szalapski, and D. Zeppenfeld, Phys. Lett. **B 283** (1992) 353;
K. Hagiwara, S. Ishihara, R. Szalapski, and D. Zeppenfeld, Phys. Rev. **D 48** (1993) 2182;
K. Hagiwara, T. Hatsukano, S. Ishihara and R. Szalapski, Nucl. Phys. **B 496** (1997) 66.

[15] M. Bilenky, J.L. Kneur, F.M. Renard and D. Schildknecht, Nucl. Phys. **B 409** (1993) 22;
M. Bilenky, J.L. Kneur, F.M. Renard and D. Schildknecht, Nucl. Phys. **B 419** (1994) 240.

[16] I. Kuss and D. Schildknecht, Phys. Lett. **B 383** (1996) 470.

[17] G. Gounaris and C.G. Papadopoulos, DEMO-HEP-96/04, THES-TP 96/11, hep-ph/9612378.

[18] The LEP-TGC combination group, LEPEWWG/TGC/2001-01, March 2001.

[19] G. J. Gounaris, J. Layssac, and F. M. Renard, Phys. Rev. **D62** (2000) 073013.

[20] G. Bélanger and F. Boudjema, Phys. Lett. **B 288** (1992) 201.

[21] J. W. Stirling and A. Werthenbach, Eur. Phys. J. **C14** (2000) 103.

[22] ALEPH Collaboration, *Limits on anomalous neutral gauge couplings using data from ZZ and $Z\gamma$ production between 183-208 GeV*, ALEPH 2001-061 (July 2001) CONF 2001-041.

[23] DELPHI Collaboration, *Study of Trilinear Gauge Boson Couplings ZZZ, $ZZ\gamma$ and $Z\gamma\gamma$*, DELPHI 2001-097 (July 2001) CONF 525.

[24] L3 Collaboration, M. Acciari *et al.*, Phys. Lett. **B 436** (1999) 187;
L3 Collaboration, M. Acciari *et al.*, Phys. Lett. **B 489** (2000) 55;
L3 Collaboration, *Search for anomalous ZZg and Zgg couplings in the process ee→Zg at LEP*, L3 Note 2672 (July 2001).

[25] OPAL Collaboration, G. Abbiendi *et al.*, Eur. Phys. J. **C 17** (2000) 13.

[26] See references [36–38].

[27] See references [39, 40].

[28] ALEPH Collaboration, *Constraints on Anomalous Quartic Gauge Boson Couplings*, ALEPH 2003-009 CONF 2003-006.

[29] L3 Collaboration, *The* $e^+e^- \to Z\gamma\gamma \to q\bar{q}\gamma\gamma$ *Reaction at LEP and Constraints on Anomalous Quartic Gauge Boson Couplings*, Phys. Lett. **B 540** (2002) 43.

[30] OPAL Collaboration, *Constraints on Anomalous Quartic Gauge Boson Couplings using Acoplanar Photon Pairs et LEP-2*, OPAL Physics Note PN510.

[31] R. Brunelière *et al.*, Phys. Lett. **B 533** (2002) 75 and references therein.

[32] J. Alcaraz, *A proposal for the combination of TGC measurements*, L3 Note 2718.

[33] R. Brunelière, *Tests on the LEP TGC combination procedures*, ALEPH 2002-008 PHYS-2002-007 (2002).

[34] O.Klein, *On the Theory of Charged Fields*, New Theories in Physics, Proceedings, Warsaw, 1938; reprinted in: Surveys of High Energ. Phys. **5** (1986) 269.

[35] L.Maiani and P.M.Zerwas, *W Static ELM Parameters*, Memorandum to the TGC Combination Group (1998).

[36] L3 Collaboration, M. Acciarri *et al.*, Phys. Lett. **B450** (1999) 281. The Z-pair cross-section at 183 GeV therein follows the L3 definition: the corresponding NC02 cross-section is given in [41].

[37] L3 Collaboration, M. Acciarri *et al.*, Phys. Lett. **B465** (1999) 363.

[38] L3 Collaboration, Ł3 Note 2805, EPS 2003 abstract 228.

[39] OPAL Collaboration, G. Abbiendi *et al.*, Phys. Lett. **B476** (2000) 256.

[40] OPAL Collaboration, CERN–EP/2003–049 submitted to Eur. Phys. J. C.

[41] Ł3 Collaboration, Ł3 Note 2366, submitted to the Winter 1999 Conferences.